ECASIA special issue paper

SURFACE and INTERFACE ANALYSIS

Received: 5 November 2013 Revised: 28 February 2014 Accepted: 3 March 2014 Published online in Wiley Online Library: 2 April 2014

(wileyonlinelibrary.com) DOI 10.1002/sia.5502

Surface and interface investigation of electrochemically induced corrosion on a quaternary bronze†

O. Papadopoulou,[a]* M. Delagrammatikas,[a] P. Vassiliou,[a] S. Grassini,[b] E. Angelini[b] and V. Gouda[c]

A quaternary (Cu-Zn-Sn-Pb) cast bronze was submitted to an electrochemical corrosion experiment using an anodic polarization sweep. The surface/interface chemical analysis of the patina removed after the anodic polarization and the metallographic observations on the corroded bulk alloy highlight the onset of a dezincification process followed by a decuprification process, as well as the formation of a Sn-enriched layer located at the interface patina-bulk alloy. Different local corrosion patterns, as CuCl precipitation in pits, epitaxial growth of corrosion products on dendritic structures and of Cl-enriched oxyhydroxides, are observed too. The results are discussed in comparison with experimental findings obtained in previous ageing tests performed on the same alloy in different chloride-containing solutions. Copyright © 2014 John Wiley & Sons, Ltd.

Keywords: metallic artefacts; corrosion; conservation; bronze; polarization curves

Introduction

Understanding the complex and heterogeneous corrosion processes, which threaten metallic cultural heritage artefacts, is a prerequisite for the design of tailored conservation protocols.[1–6] Copper-based alloys are more vulnerable to chloride attack compared to other corrosive species, especially when they are exposed to marine or coastal environment or during burial in Cl^- enriched soils. Artefacts are mainly endangered by 'bronze disease' when the pitting corrosion is developed at high %RH and chloride supply.[7–10] Moreover, phase segregation phenomena contribute to surface heterogeneity and induce local galvanic cells.[11–16] The binary Cu-Sn bronzes exhibit selective dissolution of copper,[11] the brasses with a Zn content above 14 wt% are prone to dezincification,[9] while Pb, when present, is immiscible with alloy phases leading to rapid local corrosion and formation of passive compounds.

This work aims to simulate the electrochemical corrosion of an ancient-like cast bronze in the presence of chlorides and to evaluate the contribution of the alloying elements and of the dendritic segregation to the evolution of corrosion processes. The investigation describes the results of metal dissolution processes, the interaction of metal cations with Cl^- and O^{2-} species under the action of both charge and mass transfer processes.

Experimental techniques

The experiments were carried out on specimens of a quaternary bronze, of the following chemical composition: wt%: Cu 82, Zn 14, Sn 3.5 and Pb 0.5. The alloy, produced by casting,[17] is particularly interesting for studies in the cultural heritage field because its chemical composition and its microstructure are similar to the ones of ancient metallic artefacts.

A chloride-rich patina was formed electrochemically on the polished surface of the specimens, in aerated 0.1 M NaCl aqueous solution, at pH = 6.3, with the following electrochemical setup: a three-electrode cell, with the metal specimen as a static working electrode, a saturated calomel electrode as reference and a Pt wire as counter electrode. The volume of the electrolyte volume was 2 dm^3, and the sweep was carried out without the addition of any buffer solution or stirring. An electrochemical polarization device GAMRY (Gamry Instruments, Warminster, PA, USA) CMS 100 was employed for the patina synthesis. The specimens, after 30 min at open circuit potential conditions, were anodically polarized up to +1400 mV/E_{oc} at a scan rate of 0.25 mV/s. The experiment was monitored by regular electrolyte pH measurements and digital photography (1 snapshot/min).

The *ex situ* microchemical and morphological analysis was performed by optical microscopy using bright field and polarized light and by means of SEM (FEI Quanta 200) coupled with energy dispersive spectrometry (EDS). The patina was removed with an adhesive tape and analysed both at the interface with the electrolyte and at the interface with the bulk alloy, in order to

* *Correspondence to: O. Papadopoulo, Laboratory of Physical Chemistry, School of Chemical Engineering, National Technical University of Athens, 9 Iroon Polytechniou street, 15780, Athens, Greece.*
E-mail: olpap@central.ntua.gr

† *Paper published as part of the ECASIA 2013 special issue.*

a *Laboratory of Physical Chemistry, School of Chemical Engineering, National Technical University of Athens, 9 Iroon Polytechniou street, 15780, Athens, Greece*

b *Department of Applied Science and Technology Politecnico di Torino, Corso Duca degli Abruzzi 24, 10129, Torino, Italy*

c *National Research Centre, El-Tahir Street Dokki, 12622, Cairo, Egypt*

obtain information on the composition of the patina itself and on the stratification of the corrosion products.

Results and discussion

Electrochemically induced corrosion and surface reactions

The recorded polarization curve, shown in Fig. 1, is discussed in combination with the synchronized photographic documentation of the alloy surface, shown in Fig. 2. After 30 min immersion in open circuit conditions, the electrode surface is mainly covered by cuprous oxide, Cu_2O, on the Cu-rich phases as well as by Zn and Sn oxides, whose formation is favoured at pH = 6.3. No other additional alteration may be observed at the beginning of the anodic sweep.

As the potential increases, charge transfer phenomena control the process, and the curve exhibits a Tafel region (snapshot 2). The Cl^- ions react with Cu to form nantokite, CuCl, that, at low concentrations, gives rise to a transparent pale yellow layer, difficult to be distinguished macroscopically and partially soluble. Zn and Sn chlorides are very soluble and, when formed, soon dissolve in the electrolyte. After the first peak, the current drops, the mass transfer phenomena acquire an important role (snapshot 3) favouring an evident hydrogen evolution reaction on the counter electrode, Fig. 2(b).

As shown in Fig. 2(e), an increasing etching effect involves the entire surface of the electrode, from the border towards the centre, due to the epitaxial formation of different corrosion products on the macro-segregated alloy phases.

The appearance of the electrode surface in the middle of the second anodic dissolution region is shown in Fig. 2(c); the pH increases to 9.4. An intense selective copper migration, a decuprification process, begins to take place from the interface bulk alloy/patina through the corrosion layers. Cu^+ and Cu^{2+} species are deposited on the surface, firstly in the interdendritic areas and then above the previously formed corrosion products. The dealloying process goes on, covering a wider surface. Snapshot 6 corresponds to a maximum of the current density. Then the current density gradually decreases, reaching a passivation plateau. The oxidation of the bulk alloy becomes prevalent on the migration of Cl^- from the electrolyte towards the interface bulk alloy/patina. As shown in Fig. 2(f), the electrode surface is entirely rebuilt and covered by a dark purple-red patina. At the end of the anodic sweep, the pH reaches the value 10.3.

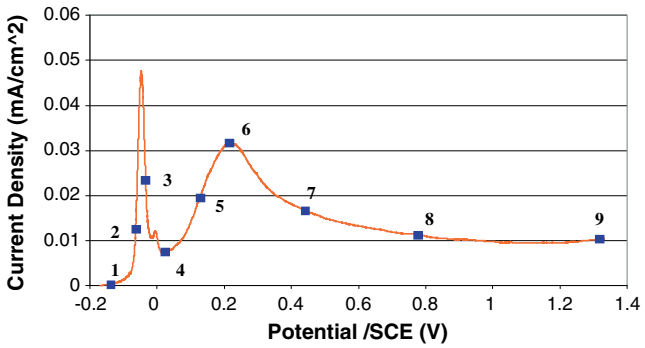

Figure 1. Anodic polarization curve recorded on the quaternary bronze in aerated 0.1 M NaCl, (scan rate = 0.25 mV/s). The numbering corresponds to the snapshots of the electrode surface, shown in Fig.2.

Microchemical and morphological characterization of the patina

The microchemical and morphological analysis allows to clarify the previously described surface reactions.

Table 1 shows the EDS data obtained on both sides of the patina removed from the alloy at the end of electrochemical experiment. Similar concentrations of Cu and Cl are found on both sides of the patina, indicating the presence of nantokite, CuCl. Dealing with the interface patina-bulk alloy, the noteworthy oxygen concentration may be mainly attributed to the presence of amorphous hydrated tin oxyhydroxides. The backscattered SEM image of the interface patina – bulk alloy, shown in Fig. 3, evidences a chemical homogeneity of the corrosion products layer, which does not fit with the chemical heterogeneity of the metallic substrate. A possible explanation may be found in the repeated dissolution and reprecipitation of the corrosion products, which can modify the initial composition of the patina, due to metal cations migration phenomena.

The different concentrations of the elements between the bulk alloy/patina and the patina/solution interface at the end of the anodic polarization test indicate that Zn and Cu cations diffuse through a layer consisting of the initially formed Cu, Zn and Sn oxides at the beginning of the electrochemical corrosion and later on through complex chlorinated oxyhydroxides as reported also by other Authors.[18,19]

In order to have a deep insight in the dealloying processes taking place on the quaternary bronze, in Table 2, the alloying elements concentrations are expressed as percentages with respect the bulk alloy composition.

At the alloy interface, a noticeable enrichment in Sn and a total depletion of Zn with respect to the substrate composition may be observed in the EDS data shown in Table 2. At the external surface of the corrosion layer, the decrease of the Zn concentration and the low percentage of Sn indicate that, at the end of the electrochemical test, almost all the residual corrosion products, which were firstly produced, are being dissolved. The Zn depletion may be attributed to a dezincification process, as a matter of fact, zinc chlorides are highly soluble and Zn, when present in concentration >14%, show a high tendency to migration. The dezincification is followed by a decuprification process; the Cu content increases from bulk alloy towards the external surface. As a final observation, Pb is not detected among the corrosion products.

In order to understand the local corrosion patterns attributed to macro-segregation phenomena, an optical examination of the patina after the electrochemical test has been performed. Figures 3(b,c) and 4(a,b,c) show the optical images of the patina surface exposed to the electrolyte and the bulk surface after the removal of the patina itself. The epitaxial growth of the corrosion products on the dendritic structure is evident on the surface patina in contact with the bulk alloy, dark and red copper oxides cover the interdendritic regions, as shown in Fig. 3(b). The corrosion products precipitated inside and around the pits developed on the alloy surface, as the one shown in Fig. 3(c), are mainly constituted by nantokite, yellow or pale yellow, often mixed with tin hydrated oxyhydroxides.

In bright field optical images, the segregated phases of the metal substrate are evidenced by the characteristic metallic hues of the predominant alloying elements. In Fig. 4(a), the interiors of the dendrites appear enriched in Sn and Zn, while the Cu-enriched interdendritic regions are subjected to extensive pitting. The polarized light optical image of the same area, shown in Fig. 4(b), better evidences the nature of the corrosion products: cuprite,

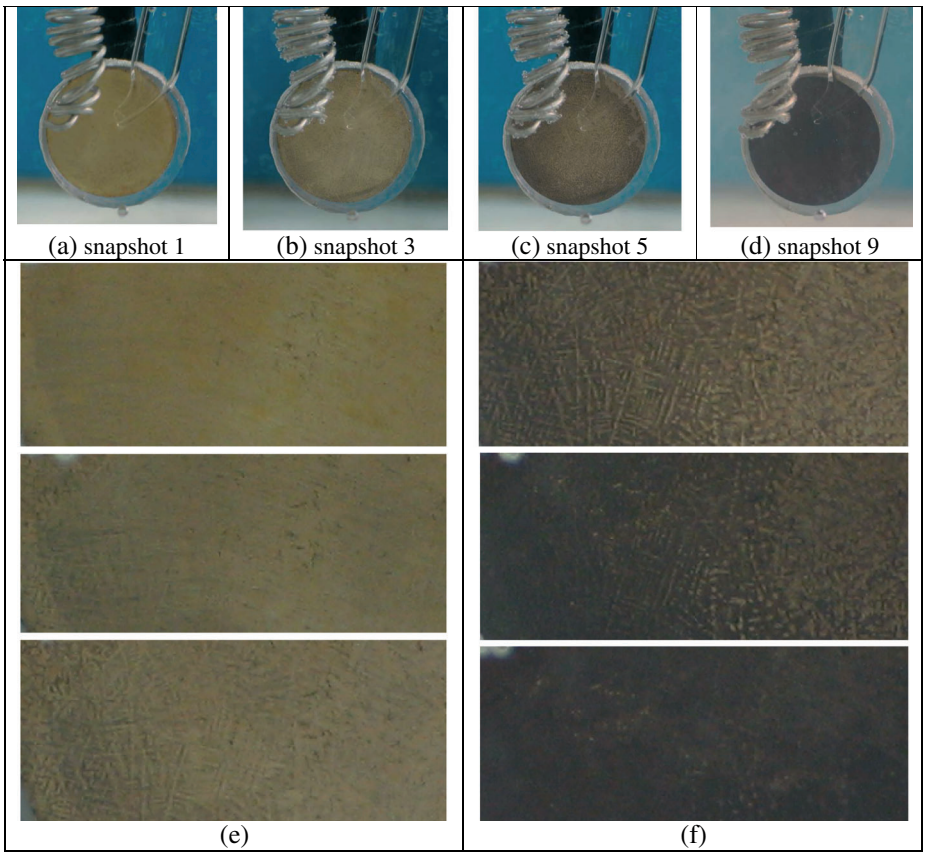

Figure 2. Optical images of selected snapshots of the three-electrode cell showing the evolution of the corrosion layers on the quaternary bronze specimen during the anodic polarization sweep shown in Fig.1: (a) snapshot 1; (b) snapshot 3; (c) snapshot 5; (d) snapshot 9; (e) optical images of the alloy surface at snapshots 2, 3 and 4; and (f) optical images of the alloy surface at snapshots 5, 6 and 7.

Table 1. EDS analysis of the patina developed on the quaternary bronze sample after the anodic polarization test. Elements concentrations expressed in Atomic %

Element	Patina surface exposed to electrolyte	Patina surface in contact with the bulk alloy
O	7.4	23.4
Cl	43.0	35.7
Sn	0.5	3
Cu	48.3	37.9
Zn	0.8	—
Pb	—	—

EDS, energy dispersive spectrometry.

Cu_2O, can be distinguished by its orange colour, while Cu oxychlorides or hydroxides appear green or blue. In Fig. 4(c), a Cu-rich, flower-shaped, region is evidenced, nantokite, CuCl, may be observed at the edges of the petals, because of its yellow colour.

The experimental findings of this study are particularly interesting if compared with the ones obtained by the Authors in previous papers,[20,21] where accelerated corrosion tests were performed on the same Cu-Zn-Sn-Pb alloy in different aggressive chloride media. The chemical corrosion process was a two-step process. In the first step, the quaternary bronze was immersed, in a 1 M $CuCl_2$ aqueous solution for 72 h, sealed from the atmosphere. In the second step, the specimen was sealed in a container in 100% relative humidity (%RH) for an incubating period of 72 h that led to the formation of corrosion products typically related to *bronze disease*. During the immersion in $CuCl_2$ solution, the Zn-bronze undergoes selective dissolution of Zn, probably in the form of $ZnCl_2$, which is highly soluble in water. After the 72 h incubation period in 100%RH, a green powdery, compact patina of poor adhesion is formed. The chemical analysis reveals that $Cu_2(OH)_3Cl$ compounds predominate over Zn, Sn and Pb corrosion compounds, rendering the bulk metal more vulnerable to chloride attack.

Both the electrochemical corrosion tests in 0.1 M NaCl solution, object of this investigation, and the chemical corrosion tests of immersion in 1 M $CuCl_2$ solution[20] result in a similar chemical composition of the patina at the interface with the electrolyte. These experimental data allow to state that, after an initial period, the electrochemical nature of the corrosion process changes in favour of the chemical reactions, when the slow processes of diffusion of anions and cations take the control of the overall corrosion process. This model satisfactorily describes the corrosion phenomena occurring on copper-based artefacts of artistic and archaeological interest subjected to marine corrosion or long-term wetting in coastal environment.

On the contrary, the degradation processes occurred during 5 years of burial in wet soil enriched with 3.5%wt NaCl[21] on quaternary bronze specimens do not allow to obtain corrosion layers of comparable composition. As a matter of fact, during

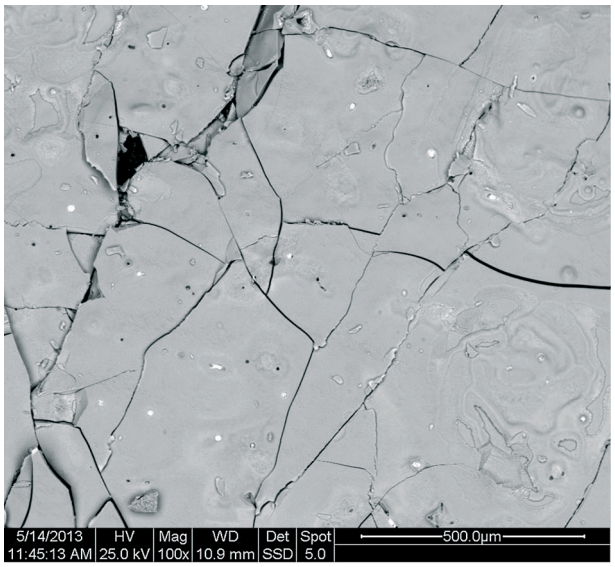

(a)

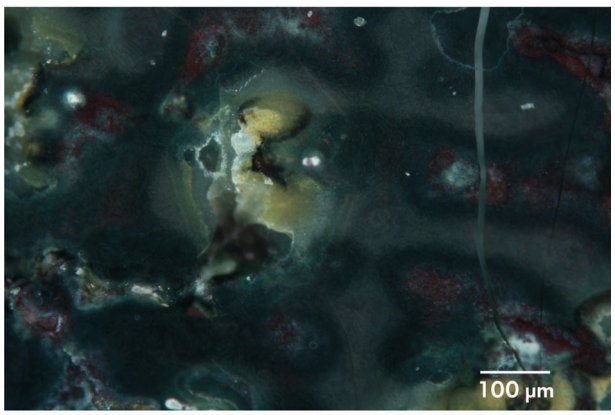

(b)

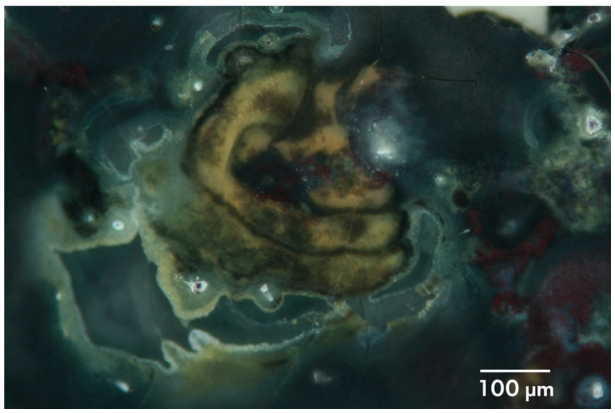

(c)

Figure 3. Patina developed on the quaternary bronze sample after the anodic polarization test. Patina surface exposed to electrolyte: (a) SEM backscattered electron image (×100); (b), (c) Optical Microscope (OM) images using polarized light (×100).

the accelerated ageing in soil, the alloy dissolution is slow and more gradual, the pH favours the formation of oxides, and soil elements create insoluble corrosion products layers that slow down the rate of dissolution of metal cations outwards as well as the incorporation of corrosive anions in the patina.

These results are of particular interest if evaluated in a common basis with the findings of the large-scale survey of the Mediterranean Basin copper-based artefacts, collected in the framework of the

Table 2. EDS analysis of the patina developed on the quaternary bronze sample after the anodic polarization test. Normalized atomic concentrations of alloying elements (%) of the both sides of the patina *versus* the bulk alloy composition

Element	Alloy	Patina surface exposed to electrolyte	Patina surface in contact with the bulk alloy
Sn	1.8	1	7.3
Cu	84.1	97.4	92.7
Zn	13.9	1.6	—
Pb	0.2	—	—

EDS, energy dispersive spectrometry.

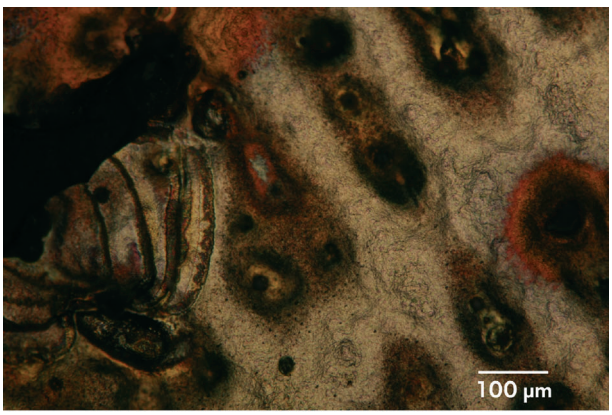

(a)

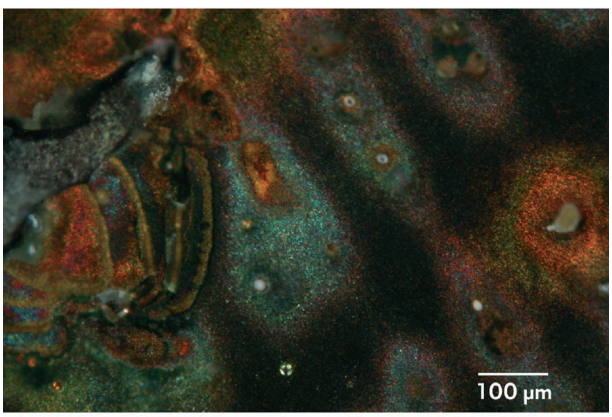

(b)

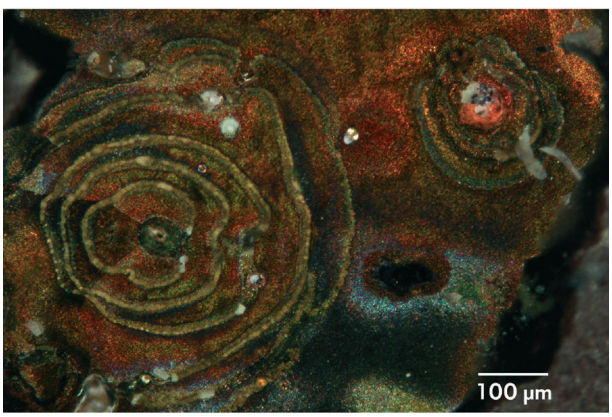

(c)

Figure 4. Bulk alloy after the removal of the patina developed on the quaternary bronze sample after the anodic polarization test. OM images (×100) showing the dendritic structure of the alloy surface using bright field (a) and polarized light (b,c).

EFESTUS project.[22] Although the case studies on artefacts with Zn content above 0.96% were rare, copper or tin depletion phenomena are commonly observed according to the microchemical investigation of the corrosion layer stratification. The presence of atacamite [$Cu_2(OH)_3Cl$], nantokite (CuCl) and piromorfite [$PbCl\ Pb_4(PO_4)_3$] has been also frequently monitored among other sulfate, phosphate and other soil constituents. X-ray diffraction has also testified to the presence of crystalline copper and tin species such as cuprite (Cu_2O), tenorite (CuO), romarkite (SnO) and cassiterite (SnO_2). It is evident that electrochemical experiments, although successfully simulate the formation of Cu species, do not allow the crystallization of many corrosion products encountered on archaeological artefacts after slow solid state diffusion processes – especially tin compounds – due to the rapid metal dissolution reactions at the metal/electrolyte interface.

Concluding remarks

The importance of the alloying elements and the metallurgical features in the corrosion evolution processes of an ancient-like quaternary bronze has been evidenced. The observation of the surface reactions during the anodic polarization in a 0.1 M NaCl solution as well as the *ex situ* characterization of the formed patina and of the corroded metal substrate has been performed. The initial epitaxial formation of stable Cu and Sn oxides at the surface and the chemical heterogeneity attributed to dendritic structures define decisively the corrosion rate and the nature of the corrosion products. A dezincification process followed by a subsequent decuprification process are observed, while the metal dissolution and the diffusion of Cl^- and O^{2-} anions take place through a Sn-enriched layer located at the alloy interface. Although at the beginning of the polarization the charge transfer rules the system reactions, in the end, the produced patina has very similar chemical composition with the one created by chemical corrosion. This proves the importance of diffusion at high potentials and pH.

Further investigations will be performed on the electrochemical and mass transport mechanisms during corrosion processes of copper-based alloys in Cl^- environment.

A wide comparison of the chemical compositions and microstructures of patinas obtained with chemical and electrochemical corrosion methods, with the ones found on aged metallic artefacts coming from different archaeological excavation sites of the Mediterranean Basin, is now running in order to understand the complex corrosion mechanisms of copper-based alloys induced by chloride ions and to design tailored conservation treatment protocols.

References

[1] A. D. Scott, Metallography and Microstructure of Ancient and Historic Metals, Getty Conservation Institute in association with Archetype Books, Singapore, **2002**.
[2] A. Mezzi, E. Angelini, C. Riccucci, S. Grassini, T. De Caro, F. Faraldi, P. Bernardini, *Surf. Interface Anal.* **2012**, *44*(8), 958.
[3] E. Angelini, F. Rosalbino, S. Grassini, G. M. Ingo, T. De Caro, in Corrosion of Metallic Heritage Artefacts: Investigation, Conservation and Prediction of Long Term Behaviour, (Eds: P. Dillmann, G. Beranger, P. Piccardo, H. Matthiensen), Woodhead Pub. Lim., Cambridge, **2007**, p. 203.
[4] G. M. Ingo, E. Angelini, G. Bultrini, I. Calliari, M. Dabala', T. De Caro, *Surf. Interface Anal.* **2002**, *34*, 337.
[5] G. M. Ingo, L. Manfredi, G. Bultrini, E. Lo Piccolo, *Archaeometry* **1997**, *39* 59.
[6] M. A. Emami, M. Bigham, *Surf. Eng.* **2013**, *29*(2), 128.
[7] O. Mircea, I. Sandu, V. Vasilache, A. V. Sandu, *Microsc. Res. Tech.* **2012**, *75*(11), 1467.
[8] V. Gouda, G. I. Youssef, N. A. A. Ghani, *Surf. Interface Anal.* **2012**, *44* (10), 1338.
[9] D. A. Scott, Copper and Bronze in Art, Corrosion, Colorants, Conservation, Getty Conservation Institute, Los Angeles, **2002**.
[10] J. Doménech-Carbó, *Solid State Electrochem.* **2010**, *14*, 349.
[11] D. Šatović, L. Valek Žulj, V. Desnica, S. Fazini ć, S. Martinez, *Corros. Sci.* **2009**, *51*, 1596.
[12] V. Costa, K. Leyssens, A. Adriaens, N. Richard, F. Scholz, *J. Solid State Electrochem.* **2010**, *14*, 449.
[13] L. Robbiola, J. M. Blengin, C. Fiaud, *Corros. Sci.* **1998**, *40*, 2083.
[14] E. Angelini, A. Batmaz, A. Cilingiroglou, S. Grassini, G. M. Ingo, C. Riccucci, *Surf. Interface Anal.* **2010**, *40*(6-7), 675.
[15] D. Walaszek, M. Senn, M. Faller, L. Philippe, B. Wagner, E. Bulska, A. Ulrich, *Spectrochim. Acta, Part B – At. Spectrosc.* **2013**, *79-80*, 17.
[16] G. M. Ingo, E. Angelini, T. De Caro, G. Bultrini, I. Calliari, *Appl. Phys. A* **2004**, *79*(2), 199.
[17] M. P. Casaletto, T. De Caro, G. M. Ingo, C. Riccucci, *Appl. Phys. A* **2006**, *2006*(83), 617.
[18] C. Debiemme-Chouvy, F. Ammeloot, E. M. M. Sutter, *Appl. Surf. Sci.* **2001**, *174*, 55.
[19] L. Robbiola, T. T. M. Tran, P. Dubot, O. Majerus, K. Rahmouni, *Corros. Sci.* **2008**, *50*, 2205.
[20] O. Papadopoulou, J. Novakovic, P. Vassiliou, E. Filippaki, Y. Bassiakos, *Appl. Phys. A: Mater. Sci. Process.* **2013**, *113*(4), 981.
[21] J. Novakovic, O. Papadopoulou, M. Delagrammatikas, P. Vassiliou, E. Filippaki, C. Xaplanteris, Y. Bassiakos, Proc. 29th International Conference on Corrosion Mitigation and Surface Protection Technologies, Alexandria/ Egypt, **2010**.
[22] G. M. Ingo, T. DeCaro, C. Riccucci, E. Angelini, S. Grassini, S. Balbi, P. Bernardini, D. Salvi, L. Bousselmi, A. Cilingiroglu, M. Gener, V. K. Gouda, O. Al Jarrah, S. Khosroff, Z. Mahdjoub, Z. Al Saad, W. El-Saddik, P. Vassiliou, *Appl. Phys. A* **2006**, *83*(4), 513.